

1
2
3
4
5
6
7
8
9
10
11

Pervasive foreshock activity across southern California

Daniel T. Trugman¹, Zachary E. Ross²

¹ Geophysics Group, Earth and Environmental Sciences Division, Los Alamos National Laboratory, Los Alamos NM

²Seismological Laboratory, California Institute of Technology, Pasadena CA

Corresponding author: Daniel Trugman (dtrugman@lanl.gov)

12 **Abstract**

13 Foreshocks have been documented as preceding less than half of all mainshock
14 earthquakes. These observations are difficult to reconcile with laboratory earthquake
15 experiments and theoretical models of earthquake nucleation, which both suggest that foreshock
16 activity should be nearly ubiquitous. Here we use a state-of-the-art, high-resolution earthquake
17 catalog to study foreshock sequences of magnitude M4 and greater mainshocks in southern
18 California from 2008-2017. This highly complete catalog provides a new opportunity to examine
19 smaller magnitude precursory seismicity. Seventy percent of mainshocks within this catalog are
20 preceded by foreshock activity that is significantly elevated compared to the local background
21 seismicity rate. Foreshock sequences vary in duration from several days to weeks, with a median
22 of 16.6 days. The results suggest that foreshock occurrence in nature is more prevalent than
23 previously thought, and that our understanding of earthquake nucleation may improve in tandem
24 with advances in our ability to detect small earthquakes.

25 **1 Introduction**

26 There has long been an underlying tension between two competing observations of
27 earthquake occurrence. From one perspective, the occurrence of large earthquakes within a fault
28 zone appears random in time, and indeed classical models of earthquake hazard are based on a
29 Poisson process that encodes this random, memoryless behavior by assumption (Baker, 2013). In
30 contrast, one of the most striking characteristics of earthquakes is that they tend to cluster in
31 space and time, with the triggering of aftershocks following larger, mainshock earthquakes being
32 the best-studied example. The physical mechanisms driving aftershock occurrence are
33 reasonably well-understood, at least a high level: slip on the mainshock fault interface imparts
34 both static (King et al., 1994; Lin & Stein, 2004; Stein, 1999) and dynamic (Brodsky, 2006;
35 Gomberg & Davis, 1996; Kilb et al., 2000; Velasco et al., 2008) stress changes in Earth's crust
36 that trigger aftershock activity. Postseismic fault slip, subcrustal viscoelastic relaxation, and
37 poroelastic stress transfer may also play an important role in certain circumstances (Freed, 2005;
38 Freed & Lin, 2001; Koper et al., 2018; Ross et al., 2017).

39 Foreshocks – earthquake occurrences preceding mainshocks – are less well understood.
40 While it is unambiguous that foreshocks do occasionally occur, both their physical significance
41 and their relative prevalence are subject to vigorous debate (Ellsworth & Bulut, 2018; Seif et al.,

42 2019; Shearer & Lin, 2009; Tape et al., 2018). In laboratory earthquake experiments, precursory
43 slip events analogous to foreshocks are observed in nearly all instances (Bolton et al., 2019;
44 Johnson et al., 2013; Rouet-Leduc et al., 2017; W. Goebel et al., 2013). Likewise, theoretical
45 models of fault friction, including the widely used rate-and-state framework, typically require a
46 seismic nucleation phase preceding dynamic rupture (Ampuero & Rubin, 2008; Dieterich, 1994;
47 Marone, 1998). These facets of laboratory and theoretical earthquake behavior suggest that
48 foreshock occurrence may be a natural manifestation of a nucleation or preslip process preceding
49 rupture (Bouchon et al., 2013; Dodge et al., 1996). This interpretation if correct would have
50 important scientific and practical consequences, and would intimate that foreshocks could
51 potentially be used to forecast characteristics of eventual mainshock occurrence.

52 One problem with this interpretation is that foreshock activity in nature is not observed as
53 frequently as it should be if it were a universal feature of earthquake nucleation. While it is
54 notoriously difficult to compare different foreshock studies due to different magnitude thresholds
55 or space-time selection windows (Reasenber, 1999), foreshocks have previously been observed
56 to precede 10-50% of mainshocks (Abercrombie & Mori, 1996; Chen & Shearer, 2016; Jones &
57 Molnar, 1976; Marsan et al., 2014; Reasenber, 1999). Taking these observations at face value,
58 what happens during the nucleation process of the other 50 to 90% of earthquakes? Are there
59 really no foreshocks, or are we simply not listening closely enough to detect them? The notion
60 that there exists undetected but substantial foreshock activity is supported by a recent meta-
61 analysis of 37 different studies of foreshocks (Mignan, 2014), which revealed systematic
62 differences in the outcome depending on the minimum magnitude of foreshock detected. A
63 similar effect can be seen in laboratory experiments, as the ability to forecast imminent
64 laboratory earthquakes depends fundamentally on the magnitude of completion of precursory
65 slip events (Lubbers et al., 2018).

66 In this study, we measure foreshock activity using a powerful new tool: a state-of-the-art
67 earthquake catalog (Ross et al., 2019) of more than 1.81 million earthquakes that occurred in
68 southern California from 2008 through 2017. The extraordinary detail of this catalog, which is
69 complete regionally down to M0.3 and locally down M0.0 or less, allows us to examine
70 precursory seismicity at the smallest of scales, in direct analog to well-recorded laboratory
71 experiments. We find that elevated foreshock activity is pervasive in southern California, with
72 70% of earthquake sequences exhibiting a significant, local increase in seismicity rate preceding

73 the mainshock event. The spatiotemporal evolution of these sequences is diverse in character, a
74 fact which may preclude real-time forecasting based on foreshock activity. Nevertheless, these
75 results help bridge the gap in our understanding of precursory activity from laboratory to Earth
76 scales.

77 **2 Earthquake Catalog Data**

78 We analyze earthquake sequences in southern California derived from the Quake
79 Template Matching (QTM) earthquake catalog (Ross et al., 2019). This recently released catalog
80 of southern California seismicity from 2008 – 2017 was compiled using approximately 284,000
81 earthquakes listed in the Southern California Seismic Network (SCSN) catalog (Hutton et al.,
82 2010) as templates for network-wide waveform cross-correlation (Gibbons & Ringdal, 2006;
83 Shelly et al., 2007), yielding more than 1.81 million detected earthquakes. The vast majority of
84 these newly detected earthquakes are small in magnitude ($-2 < M < 0$), well beneath the M1.7
85 completeness threshold of the original SCSN catalog. The QTM catalog, by contrast, is more
86 than an order of magnitude more complete, with consistent detection at M0.0 and below in
87 regions of dense station coverage.

88 We examine foreshock activity for magnitude M4 and greater mainshocks located within
89 the latitude and longitude ranges of $[32.68^\circ, 36.20^\circ]$ and $[-118.80^\circ, -115.40^\circ]$. This spatial
90 boundary was guided by the density of the SCSN station coverage and the local magnitude of
91 completeness (Figure S1), since in more remote locations the template matching detection
92 threshold is poorer. The lower latitude boundary of 32.68° is set to approximate the
93 California/Mexico border, so the study region only contains events within southern California.

94 Within this study region, we select a total of 43 mainshocks that are relatively isolated in
95 space and time from other larger events, to ensure that the selected events are indeed mainshocks
96 as traditionally defined, and that the seismicity rate during the pre-event window is not biased
97 high due to aftershock triggering from unrelated events. To do this, we use a magnitude-
98 dependent windowing criterion to exclude events within (i) 40 days and 40 km another M4
99 event, (ii) 80 km, 80 days of an M5 event, (iii) 160 km, 160 days of an M6 event, or (iv) 240 km,
100 240 days of an M7 event. We note that this criteria removes a large number of potential
101 mainshocks occurring in the months following the 2010 M7.2 El Mayor-Cucapah earthquake,

102 when the high triggered seismicity rate (Hauksson et al., 2011; Meng & Peng, 2014) renders
103 foreshock analyses problematic. The El Mayor-Cucapah event is not considered in this study due
104 to its location in Baja California, to south of our study region, though it was itself preceded by a
105 notable foreshock sequence (Chen & Shearer, 2013).

106 **3 Methods**

107 For each selected mainshock, we measure the local background rate of seismicity within
108 10 km epicentral distance of the mainshock using the interevent time method (Hainzl et al.,
109 2006). In this technique, the set of observed interevent time differences τ between subsequent
110 events, are modeled as gamma distribution:

$$111 \quad p(\tau) = C \cdot \tau^{\gamma-1} \cdot e^{-\mu \tau}. \quad (1)$$

112 Here, μ is the background rate, γ is the fraction of the total events that are background
113 events, and $C = \mu^\gamma / \Gamma(\gamma)$ is a normalizing constant. The appeal of the interevent time method is
114 that it can be used to extract a background rate from temporally clustered earthquake catalog data
115 without assuming an explicit functional form for triggered, non-background seismicity as in the
116 popular epidemic type aftershock sequence (ETAS) model (Ogata, 1988). For each earthquake,
117 we solve for μ using a maximum likelihood approach (van Stiphout et al., 2012), and estimate
118 uncertainties using a log-transformed jackknife procedure (Efron & Stein, 1981).

119 Having established the local background rate, we consider potential foreshocks within
120 this same 10 km distance range from the mainshock. While most previous studies neglect the
121 local background rate and consider any earthquake sufficiently close in space and time to the
122 mainshock to be a foreshock (Abercrombie & Mori, 1996; Chen & Shearer, 2016), this
123 assumption is clearly problematic for the QTM catalog due to its high spatiotemporal event
124 density. Thus, to measure the statistical significance of foreshock activity, we count the observed
125 number of earthquakes N in the 20 days preceding the mainshock, and use Monte Carlo
126 simulations to compute the probability p of observing at least N events during the 20-day / 10-km
127 window, given the background rate μ and its uncertainty. Low p -values are indicative of

128 foreshock activity rates in excess of the background rate, and we consider $p < 0.01$ to be
129 statistically significant evidence for elevated foreshock activity.

130 These background rate estimates, when combined with the relative completeness of the
131 QTM catalog, enable measurement of the duration of significant foreshock activity, a subject that
132 has not been carefully studied to date. To do this, we calculate the event rate within 5-day
133 moving windows (and the same 10 km spatial windows). We work backwards in time from the
134 mainshock origin time $T = 0$, in steps of 0.1 days, until the observed event rate falls to within
135 one standard deviation of the background rate μ , and take the window end time to be the
136 duration estimate. We use a 5-day window (rather than, for example, 10 days or 20 days), as we
137 found it to be the best compromise between precision in defining the onset of foreshock
138 sequences, and robustness to short-duration gaps in seismicity. Measurement uncertainties in the
139 duration estimates are of order 1 day, controlled primarily by the uncertainty in the background
140 rate and the temporal averaging (5 days) used to compute the observed event rates.

141 It is also important to understand how improved catalog completeness augments our
142 understanding of foreshock sequences. This issue is pertinent both within and beyond the study
143 region of California, as future studies in regions across the globe will provide new high-
144 resolution catalogs by applying advanced event detection techniques (Kong et al., 2019; Yoon et
145 al., 2015). To address this question in southern California, we repeat our analysis of the 43
146 foreshock sequences using the SCSN catalog instead of the QTM catalog, using an identical
147 procedure to calculate background rates and compute the p -value of the observed foreshock
148 count within 20 days and 10 km (Figure S2).

149 **4 Results**

150 In total, 30 out of 43 mainshocks in southern California have a statistically significant
151 increase in foreshock activity relative to the background seismicity rate (Figure 1 and Table S1).
152 This 70% fraction suggests that precursory seismicity is more ubiquitous than previously
153 understood, and that the discrepancy between the prevalence of foreshocks in laboratory and real
154 Earth studies may in part be explained by observation limitations. This hypothesis is supported
155 through direct comparison with the SCSN catalog, in which only 21 of the 43 sequences exhibit

156 significant foreshock activity. This fraction is consistent with recent studies of foreshocks in
157 California (Chen & Shearer, 2016), which helps validate our methodology.

158 The improvement in the resolution of foreshock sequences using the QTM catalog is
159 particularly notable given that the SCSN catalog with a nominal magnitude of completeness of
160 M1.7, is among the highest quality network-based catalogs currently available. Despite this,
161 there are numerous cases in which the SCSN catalog misses foreshock sequences entirely
162 (Figures 2 and 3). In other instances where foreshock activity is apparent in both catalogs, the
163 QTM catalog provides improved detail of the low-magnitude foreshock events that provide a
164 more complete perspective of the nucleation process. For example, in the earthquake sequences
165 depicted in Figure 4, the precise timing of the onset of each foreshock sequence is readily
166 apparent using the QTM catalog, but is impossible to discern using the SCSN catalog alone.

167 The QTM catalog also provides a unique opportunity to examine the spatial and temporal
168 characteristics of foreshock sequences in southern California. We can, for example, estimate the
169 duration of foreshock activity by measuring the timespan preceding the mainshock for which the
170 pre-event seismicity rate significantly exceeds the background rate (Figures 2-4, see Methods).
171 Estimated foreshock durations for the 30 sequences range in length from 3 to 35 days, with a
172 median of 16.6 days (Table S1). The duration estimates are limited in their precision by the
173 uncertainty in the background rate and the temporal averaging required to compute the observed
174 event rate. However, with nominal uncertainties of order 1 day, they still provide a useful
175 measure of the temporal extent of elevated foreshock activity.

176 The foreshock sequences are diverse in their spatiotemporal evolution. Many of the
177 longer-duration sequences are earthquake swarms that have been previously documented in
178 select regions of southern California (Zhang & Shearer, 2016). A number of mainshocks are
179 preceded by burst-like foreshock sequences near the mainshock hypocenter in the days and hours
180 leading up to the event, while still others have a more diffuse and widespread elevation in
181 seismicity rate (Figure 4 and Figure S3). Likewise, there are some notable instances of
182 systematic linear migration in foreshocks toward the mainshock hypocenter, but this behavior is

183 not universally observed. Indeed, these sequences exemplify the diverse characteristics one
184 might anticipate in complex natural fault systems.

185 We do not observe variations in foreshock behavior related to mainshock magnitude or
186 focal mechanism type, and the slight trend for shallow mainshocks to have more intense
187 foreshock activity is not statistically significant given our relatively small sample size of
188 candidate mainshocks (Figure S4). These findings may in part be attributed to the relative
189 homogeneity in tectonic regime of the study region of southern California (Reasenber, 1999).
190 There are, however, subtle regional differences in foreshock activity. For example, the
191 earthquake sequences nearest the Salton Sea and Coso geothermal field all feature extensive
192 foreshock activity, while several well-recorded sequences near coastal Los Angeles do not
193 (Figure 1). We note that at least two of the sequences without significant foreshock activity are
194 within a remote part of the Eastern California Shear Zone with relatively sparse station coverage,
195 so it is possible that smaller magnitude foreshocks in those particular sequences went undetected.
196 Further, our significance criterion of $p < 0.01$ is conservative by design, and thus selects only the
197 most robustly observed foreshock sequences. There are six additional sequences with $0.01 < p <$
198 0.1 in which the observed seismicity rates exceed the inferred background rate, but not to the
199 extent where the physical significance of this rate increase is unambiguous.

200 **5 Conclusions**

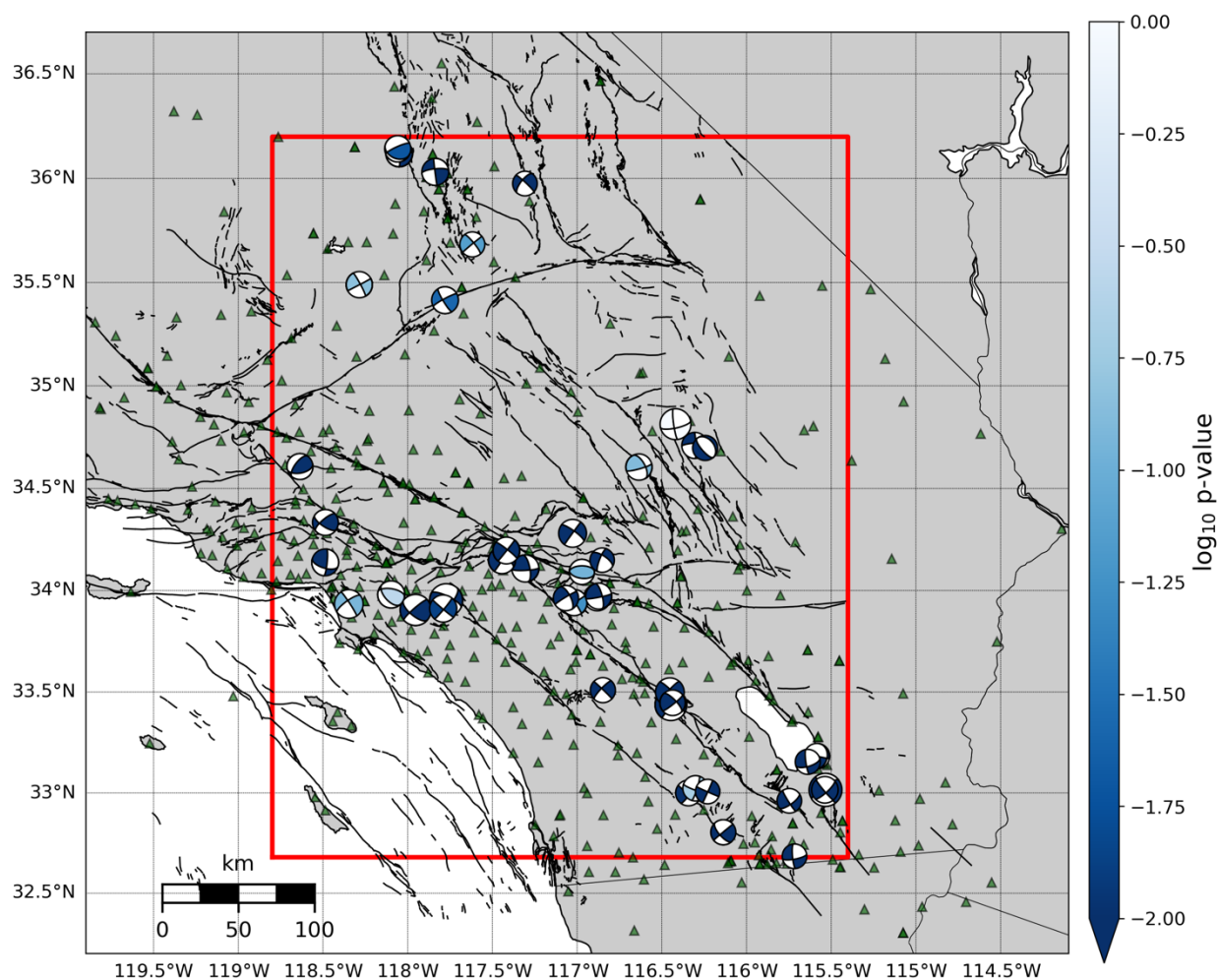
201 We use a detailed new earthquake catalog to demonstrate that elevated foreshock activity
202 is much more common than previously understood. The details of these foreshock sequences
203 have to date been obscured by limitations in catalog completeness, even in southern California,
204 where the SCSN maintains one of the most complete regional earthquake catalogs in the world.
205 The prevalence of measurable foreshock activity we observe is reminiscent of laboratory
206 experiments, where low-amplitude precursory slip events are ubiquitously observed preceding
207 failure. In the laboratory, the statistical characteristics of these slip events can be used to predict
208 the properties of imminent mainshocks, including their timing and slip amplitudes (Hulbert et al.,
209 2019; Rouet-Leduc et al., 2017).

210 Despite the notable similarities with laboratory studies, the complexity observed in the
211 real Earth will likely preclude hazard monitoring based on foreshock activity for the foreseeable

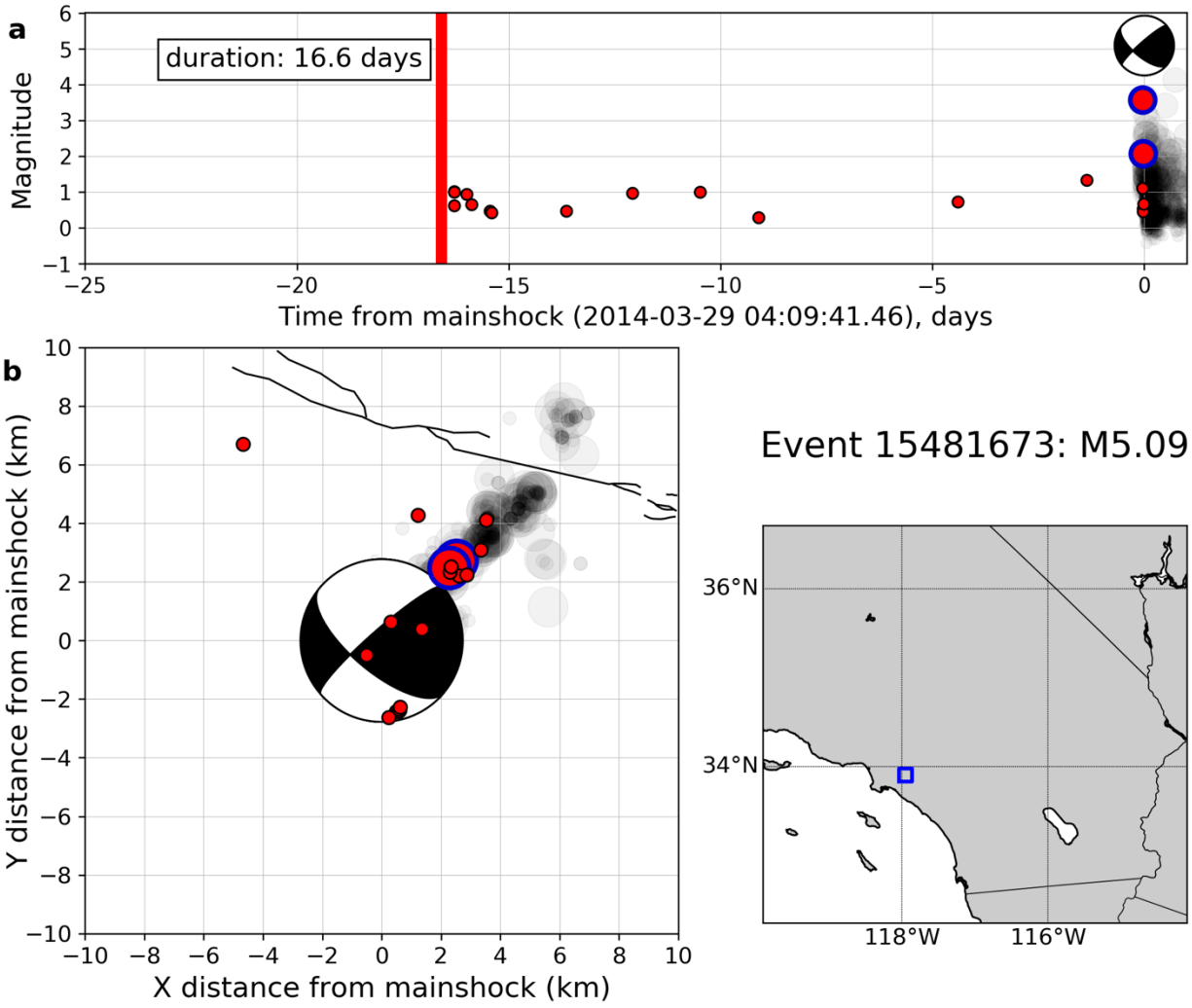
212 future. Even within the limited study region of southern California, foreshock sequences vary
213 substantially in duration and spatiotemporal evolution. Likewise, in real fault systems,
214 precursory activity is not a unique cause of elevated seismicity rates, which are more commonly
215 observed in association with aftershock triggering. While foreshock activity may be apparent in
216 retrospect after careful statistical analyses, identifying foreshocks in real time presents a whole
217 new set of challenges that we do not attempt to address in this work. It is also important to note
218 that there are several instances of well-recorded mainshock events within our catalog that occur
219 without detectable foreshocks, a fact which suggests that the nucleation processes of individual
220 earthquakes are diverse rather than universal in character. Nevertheless, by examining the details
221 of earthquake activity at the finest of scales, we will improve our understanding of the physical
222 mechanisms underlying how earthquakes get started.

223 **Acknowledgments**

224 The two earthquake catalogs analyzed in the manuscript are publicly available online.
225 The QTM catalog and the SCSN catalog are both archived by the Southern California
226 Earthquake Data Center (scedc.caltech.edu/). The workflow and statistical analysis described in
227 the Methods section was performed using open source python software packages. D. Trugman
228 acknowledges institutional support from the Laboratory Directed Research and Development
229 (LDRD) program of Los Alamos National Laboratory under project number 20180700PRD1.
230 We are grateful to P. Johnson, I. McBrearty, and N. Lubbers for their helpful advice that
231 improved the manuscript.

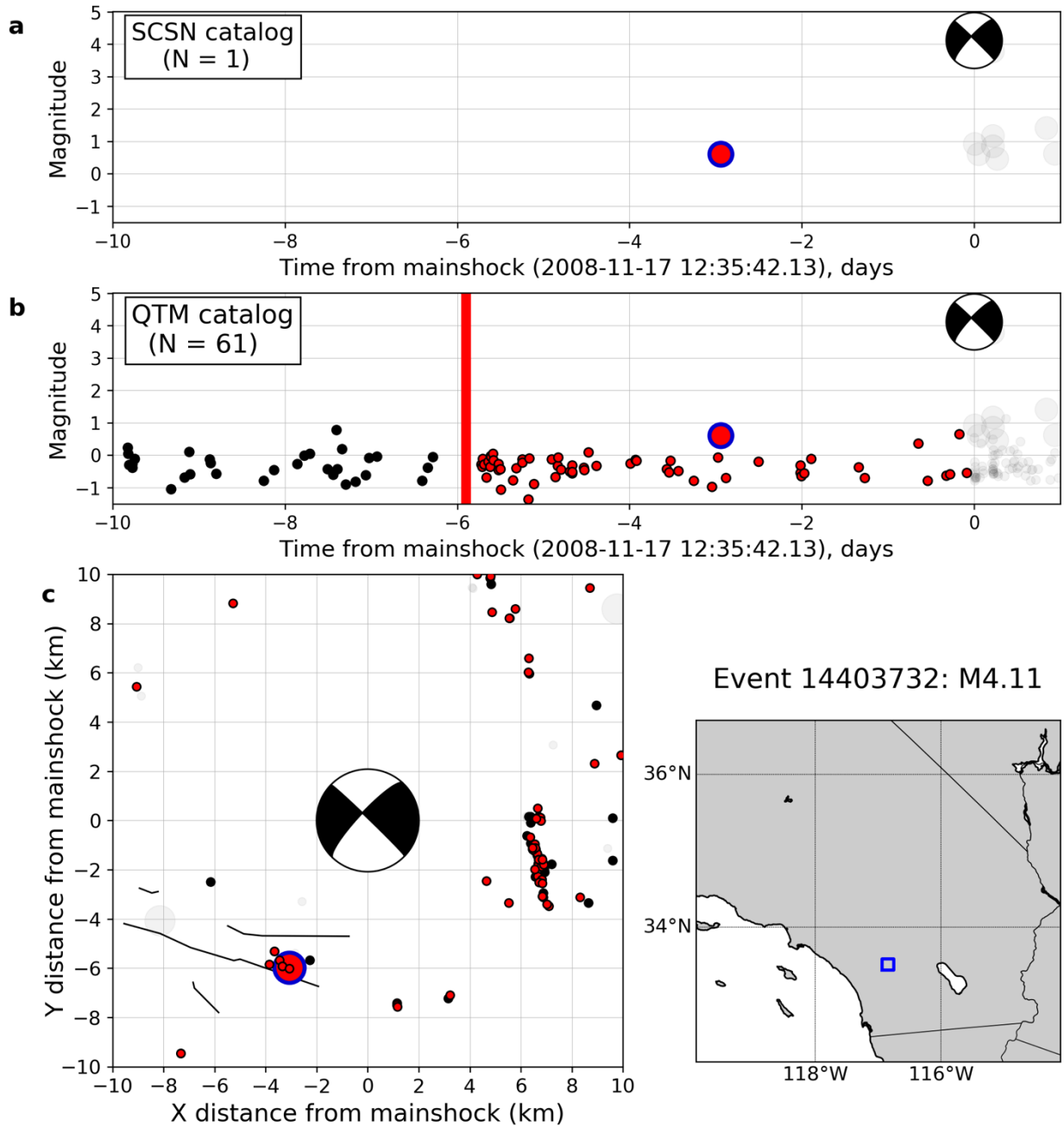


233
 234 **Figure 1.** Foreshock sequences of 43 M4 and M5 earthquakes in southern California. The study
 235 region outlined in red – $[32.68^\circ, 36.20^\circ]$ latitude and $[-118.80^\circ, -115.40^\circ]$ longitude – was
 236 selected to ensure a sufficiently low magnitude of completion for detection (Figure S1). Each
 237 event is color-coded by the p -value measurement of foreshock activity described in the text, with
 238 lower p -values (darker colors) indicating more significant activity.

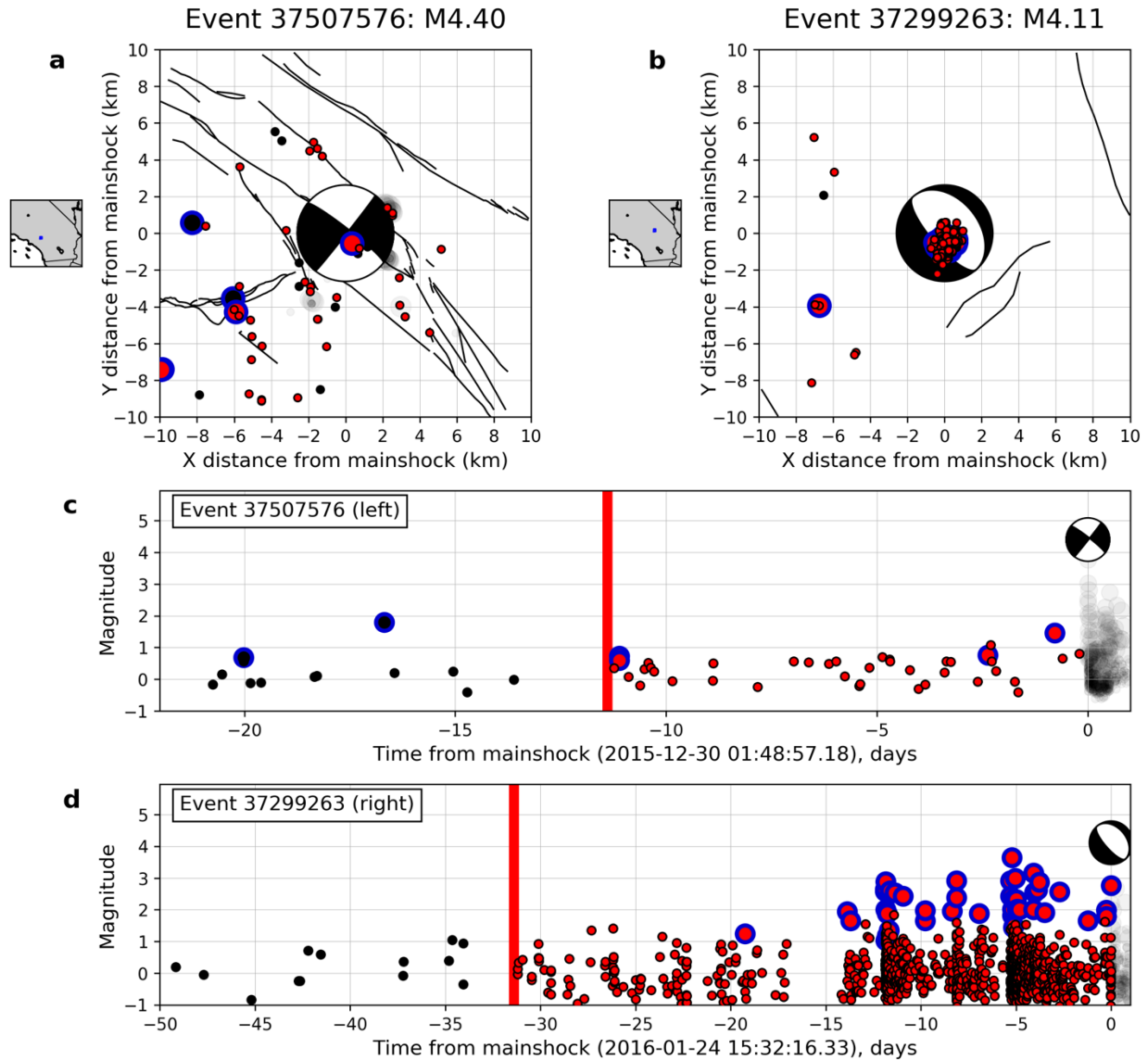


239
 240
 241
 242
 243
 244
 245

Figure 2. Example foreshock sequence for a M5.09 earthquake occurring during January 2016 (Event 15481673). (a) Earthquake magnitude versus time for events within a 10km region of the mainshock. Large circles with solid blue lines denote events listed within the SCSN catalog, while small circles denote newly detected events listed by the QTM catalog. The inferred foreshock duration of 16.6 days is denoted with a vertical red line. (b) Map view of the foreshock sequence and its location within southern California.



246
 247 **Figure 3.** Hidden foreshocks revealed by the improved detection capability of the QTM catalog.
 248 Panels (a) and (b) compare the magnitude-time evolution of the foreshock sequence for an
 249 example earthquake (Event 14403732) from the perspective of (a) the SCSN catalog (b) the
 250 QTM catalog. In the 6 days preceding this event, only one SCSN earthquake was recorded,
 251 compared to 61 in the QTM catalog. Red circles denote events following the estimated foreshock
 252 duration (red line), while black circles denote events preceding this. (c) Map view of the
 253 foreshock sequence and its location within southern California.



254
 255
 256
 257
 258
 259
 260
 261
 262
 263

Figure 4. Diverse patterns of foreshock occurrence in southern California. Panels (a) and (b) show map view representations of two distinct foreshock sequences, one (a) with an extended period of elevated seismicity rate surrounding the mainshock hypocenter, and the other (b) with several highly localized bursts of seismicity preceding the mainshock. Red circles denote events following the estimated foreshock duration (red line), while black circles denote events preceding this. Large circles with solid blue lines denote events listed within the SCSN catalog, while small circles denote newly detected events listed by the QTM catalog. (c) and (d) Event magnitude versus time for the sequences shown in panels a and b, respectively.

264 **References**

- 265 Abercrombie, R. E., & Mori, J. (1996). Occurrence patterns of foreshocks to large earthquakes in
266 the western United States. *Nature*, 381(6580), 303–307.
267 <https://doi.org/10.1038/381303a0>
- 268 Ampuero, J.-P., & Rubin, A. M. (2008). Earthquake nucleation on rate and state faults - Aging
269 and slip laws. *Journal of Geophysical Research*, 113(B1).
270 <https://doi.org/10.1029/2007JB005082>
- 271 Baker, J. W. (2013). An introduction to probabilistic seismic hazard analysis. *White Paper*
272 *Version 2.0*, 1–79.
- 273 Bolton, D. C., Shokouhi, P., Rouet-Leduc, B., Hulbert, C., Rivière, J., Marone, C., & Johnson, P.
274 A. (2019). Characterizing Acoustic Signals and Searching for Precursors during the
275 Laboratory Seismic Cycle Using Unsupervised Machine Learning. *Seismological*
276 *Research Letters*, 90(3), 1088–1098. <https://doi.org/10.1785/0220180367>
- 277 Bouchon, M., Durand, V., Marsan, D., Karabulut, H., & Schmittbuhl, J. (2013). The long
278 precursory phase of most large interplate earthquakes. *Nature Geoscience*, 6(4), 299–302.
279 <https://doi.org/10.1038/ngeo1770>
- 280 Brodsky, E. E. (2006). Long-range triggered earthquakes that continue after the wave train
281 passes. *Geophysical Research Letters*, 33(15). <https://doi.org/10.1029/2006GL026605>
- 282 Chen, X., & Shearer, P. M. (2013). California foreshock sequences suggest aseismic triggering
283 process. *Geophysical Research Letters*, 40(11), 2602–2607.
284 <https://doi.org/10.1002/grl.50444>
- 285 Chen, X., & Shearer, P. M. (2016). Analysis of Foreshock Sequences in California and
286 Implications for Earthquake Triggering. *Pure and Applied Geophysics*, 173(1), 133–152.
287 <https://doi.org/10.1007/s00024-015-1103-0>

288 Dieterich, J. (1994). A constitutive law for rate of earthquake production and its application to
289 earthquake clustering. *Journal of Geophysical Research*, 99(B2), 2601.
290 <https://doi.org/10.1029/93JB02581>

291 Dodge, D. A., Beroza, G. C., & Ellsworth, W. L. (1996). Detailed observations of California
292 foreshock sequences: Implications for the earthquake initiation process. *Journal of*
293 *Geophysical Research: Solid Earth*, 101(B10), 22371–22392.
294 <https://doi.org/10.1029/96JB02269>

295 Efron, B., & Stein, C. (1981). The Jackknife Estimate of Variance. *The Annals of Statistics*, 9(3),
296 586–596. <https://doi.org/10.1214/aos/1176345462>

297 Ellsworth, W. L., & Bulut, F. (2018). Nucleation of the 1999 Izmit earthquake by a triggered
298 cascade of foreshocks. *Nature Geoscience*, 1. <https://doi.org/10.1038/s41561-018-0145-1>

299 Freed, A. M. (2005). Earthquake triggering by static, dynamic and postseismic stress transfer.
300 *Annual Review of Earth and Planetary Sciences*, 33(1), 335–367.
301 <https://doi.org/10.1146/annurev.earth.33.092203.122505>

302 Freed, A. M., & Lin, J. (2001). Delayed triggering of the 1999 Hector Mine earthquake by
303 viscoelastic stress transfer. *Nature*, 411(6834), 180–183.
304 <https://doi.org/10.1038/35075548>

305 Gibbons, S. J., & Ringdal, F. (2006). The detection of low magnitude seismic events using array-
306 based waveform correlation. *Geophysical Journal International*, 165(1), 149–166.
307 <https://doi.org/10.1111/j.1365-246X.2006.02865.x>

308 Gomberg, J., & Davis, S. (1996). Stress/strain changes and triggered seismicity at The Geysers,
309 California. *Journal of Geophysical Research*, 101(B1), 733.
310 <https://doi.org/10.1029/95JB03250>

311 Hainzl, S., Scherbaum, F., & Beauval, C. (2006). Estimating Background Activity Based on
312 Interevent-Time Distribution. *Bulletin of the Seismological Society of America*, *96*(1),
313 313–320. <https://doi.org/10.1785/0120050053>

314 Hauksson, E., Stock, J., Hutton, K., Yang, W., Vidal-Villegas, J., & Kanamori, H. (2011). The
315 2010 Mw 7.2 El Mayor-Cucapah Earthquake Sequence, Baja California, Mexico and
316 Southernmost California, USA: Active Seismotectonics along the Mexican Pacific
317 Margin. *Pure and Applied Geophysics*, *168*(8–9), 1255–1277.

318 Hulbert, C., Rouet-Leduc, B., Johnson, P. A., Ren, C. X., Rivière, J., Bolton, D. C., & Marone,
319 C. (2019). Similarity of fast and slow earthquakes illuminated by machine learning.
320 *Nature Geoscience*, *12*(1), 69. <https://doi.org/10.1038/s41561-018-0272-8>

321 Hutton, K., Woessner, J., & Hauksson, E. (2010). Earthquake Monitoring in Southern California
322 for Seventy-Seven Years (1932-2008). *Bulletin of the Seismological Society of America*,
323 *100*(2), 423–446. <https://doi.org/10.1785/0120090130>

324 Johnson, P. A., Ferdowsi, B., Kaproth, B. M., Scuderi, M., Griffa, M., Carmeliet, J., et al. (2013).
325 Acoustic emission and microslip precursors to stick-slip failure in sheared granular
326 material. *Geophysical Research Letters*, *40*(21), 5627–5631.
327 <https://doi.org/10.1002/2013GL057848>

328 Jones, L., & Molnar, P. (1976). Frequency of foreshocks. *Nature*, *262*(5570), 677.
329 <https://doi.org/10.1038/262677a0>

330 Kilb, D., Gomberg, J., & Bodin, P. (2000). Triggering of earthquake aftershocks by dynamic
331 stresses. *Nature*, *408*(6812), 570–574. <https://doi.org/10.1038/35046046>

332 King, G. C. P., Stein, R. S., & Lin, J. (1994). Static stress changes and the triggering of
333 earthquakes. *Bulletin of the Seismological Society of America*, *84*(3), 935–953.

334 Kong, Q., Trugman, D. T., Ross, Z. E., Bianco, M. J., Meade, B. J., & Gerstoft, P. (2019).
335 Machine Learning in Seismology: Turning Data into Insights. *Seismological Research*
336 *Letters*, 90(1), 3–14. <https://doi.org/10.1785/0220180259>

337 Koper, K. D., Pankow, K. L., Pechmann, J. C., Hale, J. M., Burlacu, R., Yeck, W. L., et al.
338 (2018). Afterslip Enhanced Aftershock Activity During the 2017 Earthquake Sequence
339 Near Sulphur Peak, Idaho. *Geophysical Research Letters*, 45(11), 5352–5361.
340 <https://doi.org/10.1029/2018GL078196>

341 Lin, J., & Stein, R. S. (2004). Stress triggering in thrust and subduction earthquakes and stress
342 interaction between the southern San Andreas and nearby thrust and strike-slip faults.
343 *Journal of Geophysical Research: Solid Earth (1978–2012)*, 109(B2).

344 Lubbers, N., Bolton, D. C., Mohd-Yusof, J., Marone, C., Barros, K., & Johnson, P. A. (2018).
345 Earthquake Catalog-Based Machine Learning Identification of Laboratory Fault States
346 and the Effects of Magnitude of Completeness. *Geophysical Research Letters*, 45(24),
347 13,269–13,276. <https://doi.org/10.1029/2018GL079712>

348 Marone, C. (1998). Laboratory-Derived Friction Laws and Their Application to Seismic
349 Faulting. *Annual Review of Earth and Planetary Sciences*, 26(1), 643–696.
350 <https://doi.org/10.1146/annurev.earth.26.1.643>

351 Marsan, D., Helmstetter, A., Bouchon, M., & Dublanchet, P. (2014). Foreshock activity related
352 to enhanced aftershock production. *Geophysical Research Letters*, 41(19), 6652–6658.
353 <https://doi.org/10.1002/2014GL061219>

354 Meng, X., & Peng, Z. (2014). Seismicity rate changes in the Salton Sea Geothermal Field and the
355 San Jacinto Fault Zone after the 2010 Mw 7.2 El Mayor-Cucapah earthquake.

356 *Geophysical Journal International*, 197(3), 1750–1762.
357 <https://doi.org/10.1093/gji/ggu085>

358 Mignan, A. (2014). The debate on the prognostic value of earthquake foreshocks: A meta-
359 analysis. *Scientific Reports*, 4, 4099. <https://doi.org/10.1038/srep04099>

360 Ogata, Y. (1988). Statistical Models for Earthquake Occurrences and Residual Analysis for Point
361 Processes. *Journal of the American Statistical Association*, 83(401), 9–27.
362 <https://doi.org/10.1080/01621459.1988.10478560>

363 Reasenber, P. A. (1999). Foreshock occurrence before large earthquakes. *Journal of*
364 *Geophysical Research: Solid Earth*, 104(B3), 4755–4768.
365 <https://doi.org/10.1029/1998JB900089>

366 Ross, Z. E., Rollins, C., Cochran, E. S., Hauksson, E., Avouac, J.-P., & Ben-Zion, Y. (2017).
367 Aftershocks driven by afterslip and fluid pressure sweeping through a fault-fracture
368 mesh. *Geophysical Research Letters*, 44(16), 2017GL074634.
369 <https://doi.org/10.1002/2017GL074634>

370 Ross, Z. E., Trugman, D. T., Hauksson, E., & Shearer, P. M. (2019). Searching for hidden
371 earthquakes in Southern California. *Science*, eaaw6888.
372 <https://doi.org/10.1126/science.aaw6888>

373 Rouet-Leduc, B., Hulbert, C., Lubbers, N., Barros, K., Humphreys, C. J., & Johnson, P. A.
374 (2017). Machine Learning Predicts Laboratory Earthquakes. *Geophysical Research*
375 *Letters*, 44(18), 2017GL074677. <https://doi.org/10.1002/2017GL074677>

376 Seif, S., Zechar, J. D., Mignan, A., Nandan, S., & Wiemer, S. (2019). Foreshocks and Their
377 Potential Deviation from General Seismicity. *Bulletin of the Seismological Society of*
378 *America*, 109(1), 1–18. <https://doi.org/10.1785/0120170188>

379 Shearer, P. M., & Lin, G. (2009). Evidence for Mogi doughnut behavior in seismicity preceding
380 small earthquakes in southern California. *Journal of Geophysical Research: Solid Earth*,
381 *114*(B1). <https://doi.org/10.1029/2008JB005982>

382 Shelly, D. R., Beroza, G. C., & Ide, S. (2007). Non-volcanic tremor and low-frequency
383 earthquake swarms. *Nature*, *446*(7133), 305–307. <https://doi.org/10.1038/nature05666>

384 Stein, R. S. (1999). The role of stress transfer in earthquake occurrence. *Nature*, *402*(6762), 605–
385 609. <https://doi.org/10.1038/45144>

386 van Stiphout, T., Zhuang, J., & Marsan, D. (2012). Seismicity declustering. *Community Online*
387 *Resource for Statistical Seismicity Analysis*, *10*, 1.

388 Tape, C., Holtkamp, S., Silwal, V., Hawthorne, J., Kaneko, Y., Ampuero, J. P., et al. (2018).
389 Earthquake nucleation and fault slip complexity in the lower crust of central Alaska.
390 *Nature Geoscience*, *1*. <https://doi.org/10.1038/s41561-018-0144-2>

391 Velasco, A. A., Hernandez, S., Parsons, T., & Pankow, K. (2008). Global ubiquity of dynamic
392 earthquake triggering. *Nature Geoscience*, *1*(6), 375–379.
393 <https://doi.org/10.1038/ngeo204>

394 W. Goebel, T. H., Schorlemmer, D., Becker, T. W., Dresen, G., & Sammis, C. G. (2013).
395 Acoustic emissions document stress changes over many seismic cycles in stick-slip
396 experiments. *Geophysical Research Letters*, *40*(10), 2049–2054.
397 <https://doi.org/10.1002/grl.50507>

398 Yoon, C. E., O'Reilly, O., Bergen, K. J., & Beroza, G. C. (2015). Earthquake detection through
399 computationally efficient similarity search. *Science Advances*, *1*(11), e1501057.
400 <https://doi.org/10.1126/sciadv.1501057>

401 Zhang, Q., & Shearer, P. M. (2016). A new method to identify earthquake swarms applied to
402 seismicity near the San Jacinto Fault, California. *Geophysical Journal International*,
403 205(2), 995–1005. <https://doi.org/10.1093/gji/ggw073>

404